Abstract

We present ratios of the numbers of charged antiparticles to particles (pions, kaons and protons) in Au + Au collisions at $\sqrt{s_{NN}} = 200$ GeV as a function of rapidity in the range y=0-3. While the particle ratios a midrapidity are close to unity and consistent with significant significant nuclear transparency the K^-/K^+ and $\bar{p}/p$ ratios decrease significantly at forward rapidity. An interpretation of the results within the statistical model indicates a reduction of the baryon chemical potential from $\mu_B = 120$MeV to $\mu_B \approx 25$MeV over the considered rapidity range.

PACS numbers: 25.75 Dw.

Rapidity Dependence of Charged Antiparticle-to-Particle Ratios in Au+Au Collisions at $\sqrt{s_{NN}} = 200$ GeV

I. G. Bearden[7], D. Beavis[1], C. Besliu[10], Y. Blyakhman[6], B. Budick[6], H. Bøggild[7], C. R. C

Version: RatioDraft3.03.tex, July 4, 2002

Ratios of numbers of particles to antiparticles, and in particular the rapidity dependence of such ratios are significant indicators of the dynamics of high energy nucleus-nucleus collisions [1, 2]. At the energy of $\sqrt{s_{NN}}$=200 GeV considerable transparency even in central collisions of Au ions is expected. This should lead to a flat multiplicity density as function of rapidity (y) near midrapidity, and with values near unity for the $\bar{p}/p$ and K^-/K^+ particle number ratios. Away from midrapidity the net baryon content originating from the initial nuclei is more significant and production mechanisms other than particle-antiparticle pair production play a substantial role. Therefore $\bar{p}/p$ and K^-/K^+ ratios will decrease with increasing rapidity $|y|$. Measurements of $\bar{p}/p$ ratios at 130 GeV [3, 4, 5, 6] and of pseudo rapidity distributions of charged particles at 130 GeV [7] and 200 GeV [8, 9] point to the development described above, a reminiscent of the Bjorken picture [10].

In the present letter measurements of ratios $\pi^-/\pi^+, K^-/K^+$ and $\bar{p}/p$ as a function of rapidity, transverse momentum (p_T) and collision centrality (top 20%) are presented for Au+Au collisions at $\sqrt{s_{NN}} = 200$ GeV. We measure $\langle d^2n/dp_T dy\rangle \Delta p_T \Delta y$, where the averaging is over phase space, $\Delta p_T \Delta y$. The ratios are for the normalized numbers of detected particles, including corrections as described below.

At midrapidity, the measured antiparticle to particle ratios are approaching unity, i.e. they vary between 0.75 ± 0.04 ($\bar{p}/p$), over 0.95 ± 0.05 (K^-/K^+) to 1.01 ± 0.04 (π^-/π^+). These values exceed the corresponding ratios measured for Pb+Pb reactions at ($\sqrt{s_{NN}} = 17$ GeV) by factors of about 1.8 for the kaons and by about 10 for the protons. Recent PHOBOS measurements [11] are consistent with the y=0 measurements presented here.

While the pion ratios are consistent with unity over the entire rapidity range covered, the ratios of the strange-mesons and of the baryons drop to $K^-/K^+ = 0.62 \pm 0.08$ and $\bar{p}/p = 0.27 \pm 0.03$ at $y \approx 3$. This behavior supports the idea of the formation of a nearly baryon free zone at midrapidity in the collisions, where particle production is dominated by pair creation, either at the quark level or at the hadron level. However, towards larger rapidities, the ratios become increasingly influenced by the baryon content of the original nuclei. The present work indicates an increase, at y=0, of the ratios relative to $\sqrt{s_{NN}} = 130$ GeV Au+Au collisions of about 5% for kaons and of about 17% for protons [3, 4, 5, 6].

The data were obtained with the BRAHMS detector, which consists of two independent small-aperture magnetic spectrometers, which can rotate in the horizontal plane about the nominal interaction point (IP), covering the rapidity range $-0.1 < y < 4$ for pions and $-0.1 < y < 3.4$ for protons. Details may be found in Ref. [12]. The MidRapidity Spectrometer (MRS) consists of two time projection chambers (TPC) and a magnet, for determining particle momenta. This assembly is followed by a segmented scintillator time–of–flight wall (TOFW) for particle velocity measurements with time resolution $\sigma_t \approx 75ps$. With this arrangement π-K separation is achieved up to a momentum of 2 GeV/c and K-p separation up to 4 GeV/c. The Front Forward Spectrometer (FFS) consists, in order, of a dipole magnet, a TPC, a second dipole magnet, a second TPC, a time–of–flight wall (TOF1) and a threshold gas-Cherenkov detector (C1). At small polar angles (from 2.3° to 15°), where the mean momentum of particles is large, a back section with two dipole magnets, three drift chambers, a time of flight wall (TOF2) and a ring imaging Cherenkov detector (RICH) is also used. TOF1 (at 8.6 m) and TOF2 (at 18 m) allow for K-p separation up to p=5.5 and 8 GeV/c respectively. C1 identifies pions in the range from p=3 to 9 GeV/c and the RICH allows π-K separation up to p≈25 GeV/c and K-p separation to p≈35 GeV/c.

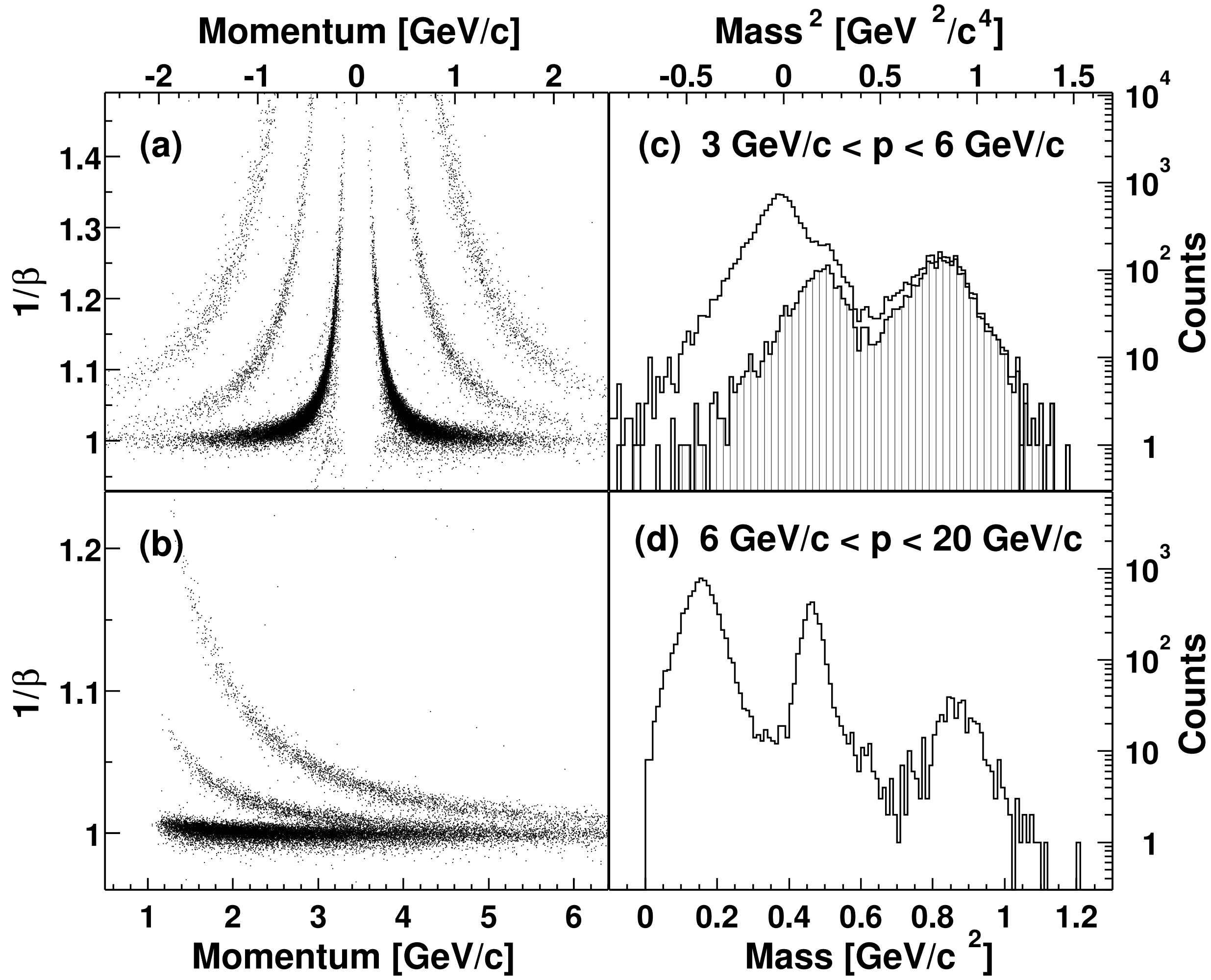

Figure 1: Particle identification capability in BRAHMS. (a) and (b) separation between pions, kaons, and protons. The MRS (a) is at 90 deg. and both charges are accepted. The FS (b) is here positioned at 12 degrees. (c) Mass-squared spectrum in the FS from time-of-flight measurements. The shaded histogram includes the vetoing of pions in C1. (d) Mass spectrum in FS utilizing the information from the RICH.

The reaction centrality was determined using a plastic scintillator tile array surrounding the intersection region [12, 7, 8]. The Beam-Beam Counters (BB) are two arrays of Cherenkov radiators positioned $\pm$ 2.15 m from the IP. They measure charged hadrons in the pseudo-rapidity range $3.0 < |\eta| < 3.8$ and, for the 25% most central collisions, they allow collision vertex determination with a resolution $\sigma_z \approx 0.65$ cm and supply the start time for the time of flight measurements with resolution $\sigma_t <= 30$ ps.

In this work the MRS was operated at 40°, 60°, and 90° and the FS at 4°,8°,12° and 20°. For magnetic fields of the same magnitude but opposite polarities, the spectrometer acceptance is identical for positively and negatively charged particles. Therefore most systematic errors associated with acceptance and detector efficiency cancel in the particle ratios. In general, the experimental methods employed here are the same as those described in [3].

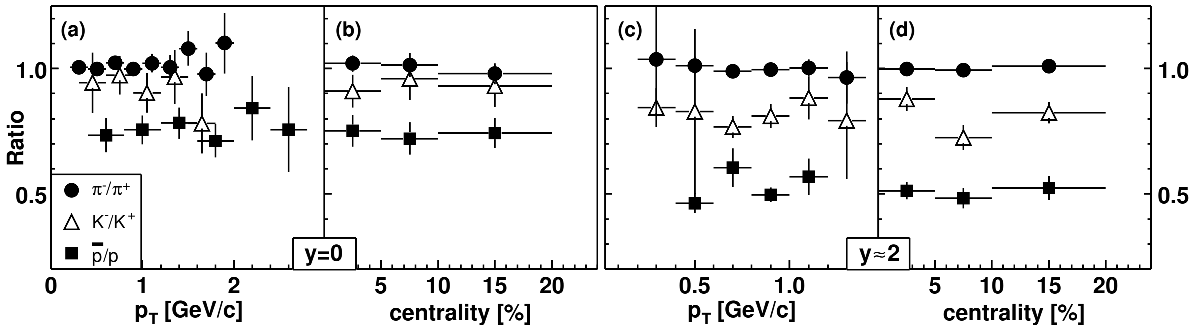

Figure 2: Dependence of the measured antihadron/hadron ratios as on transverse momentum and reaction centrality. The panels to the left are for $y = 0$ and panels to the right for high rapidities ($y_{\pi^-/\pi^+} = 2.55$, $y_{K^-/K^+} = 2.33$ and $y_{\bar{p}/p} = 2.05$).

Figure 1 shows the particle identification capability. Particle yields in the MRS and FS are determined by selecting tracks within a $\pm 2\sigma$ band of the expected β^{-1} vs. momentum for a given particle type. In the FS, additional momentum dependent cuts on the Cherenkov detector signals are applied. The number of particles measured in various runs is normalized to the number of collision events defined by the BB–ZDC coincidences fulfilling a given centrality cut. The geometrical acceptances of the spectrometers change as a function of the collision vertex and the normalization is done depending on the collision vertex, thus accounting for possible differneces in the vertex distributions from run to run. From the normalized number of antiparticles and particles the ratios are calculated.

The measured ratios have been corrected for absorption and production of secondary particles in the material traversed (Be beam tube, various detector elements and air). Losses of antiprotons due to annihilation have been evaluated in GEANT simulations to be about 3% in the MRS and 0.9% in the FS. In the MRS, the background contribution from protons arising mainly from the interaction of pions with the beam pipe, is $\approx$ 10% for the lowest p_T bin at midrapidity falling off to 2 % at p_T > 0.5GeV. In the FS this contribution is found to be negligible at the smallest angles and amounts to less than 1% at 30 degrees. For kaons decay losses cancel out, but differences in reaction cross sections for K^- and K^+ amount to less than 1%. The data have been corrected for such effects.

Figure 2 shows the dependence of the measured ratios for pions, kaons and protons (corrected as described above) on transverse momentum p_T (a and c) and collision centrality (b and d) in two selected rapidity intervals, around y=0 and $y \approx$2 respectively. The measured distributions show no significant dependence of the ratios on p_T or centrality in the covered ranges. Therefore we integrate our yields over centrality in the 0-20% range and over our accepted transverse momentum range before calculating the ratios.

The ratios shown in fig. 2 have not been corrected for protons and antiprotons that originate from weak decays of hyperons (Λ, Σ, *etc*). Corrections for feed down depend on the relative production of hyperons and primary baryons and their antiparticles, and on the respective spectrum slopes. The STAR experiment has recently measured $\Lambda/p \approx 0.5$ and $\bar{\Lambda}/\Lambda = 0.74 \pm 0.04$ at y=0 for $\sqrt{s_{NN}} = 130$ GeV collisions [16]. We have studied the magnitude of the corrections using various model assumptions as input to realistic GEANT simulations of the BRAHMS setup. Assuming primary Hyperon/Baryon ratios similar to STAR's we find that the correction to the quoted ratios in our acceptance is less than 5%.

Figure 3 shows the π^-/π^+, K^-/K^+ and $\bar{p}/p$ ratios as a function of rapidity. Statistical errors are shown as vertical error bars, while systematic plus statistical errors are indicated by the caps. Systematic uncertainties are estimated to 2% in the case of pions and kaons and to 4% in the case of protons. While the π^-/π^+ ratio is consistent with unity over the considered rapidity range, the K^-/K^+ ratio shows a decrease from 0.95 ± 0.05 at $y = 0$ to 0.62 ± 0.08 at $y = 3.05$. Likewise the $\bar{p}/p$ ratio decreases from 0.75 ± 0.04 at $y = 0$ to 0.27 ± 0.03 at $y = 2.9$. The $\bar{p}/p$ ratio at y=0 exceeds the ratio measured in Au+Au collisions at 130 GeV [3, 5, 4] by about 17%. We also note that the $\bar{p}/p$ and K^-/K^+ ratios are essentialy constant in the rapidity interval y=0-1. This is consistent with the onset of the boost invariant plateau around midrapidity proposed by Bjorken.

The measured set of particle ratios as a function of rapidity also lend itself to an analysis in terms of a model based on the assumption of a system in chemical and thermal equilibrium such as has already been advocated for SPS energies. Recently, particle ratios measured at RHIC at $\sqrt{s_{NN}} = 130$ GeV have been analyzed in a Grand Canonical Ensemble (GCE) with baryon number, strangeness and charge conservation [18].

The relevant parameters of the model are the temperature T and the baryon (or light quark) chemical potential $\mu_B = 3\mu_q$. $T = 174 \pm 7$ MeV and $\mu_B = 46 \pm 5$ MeV are found. In Ref. [18] a parametrization as a function of energy is proposed leading to a prediction for $\sqrt{s_{nn}} = 200$ GeV of $T = 177 \pm 7$ MeV, $\mu_B = 29 \pm 8$ MeV and thus $\bar{p}/p$ =0.752, K^-/K^+=0.932, and

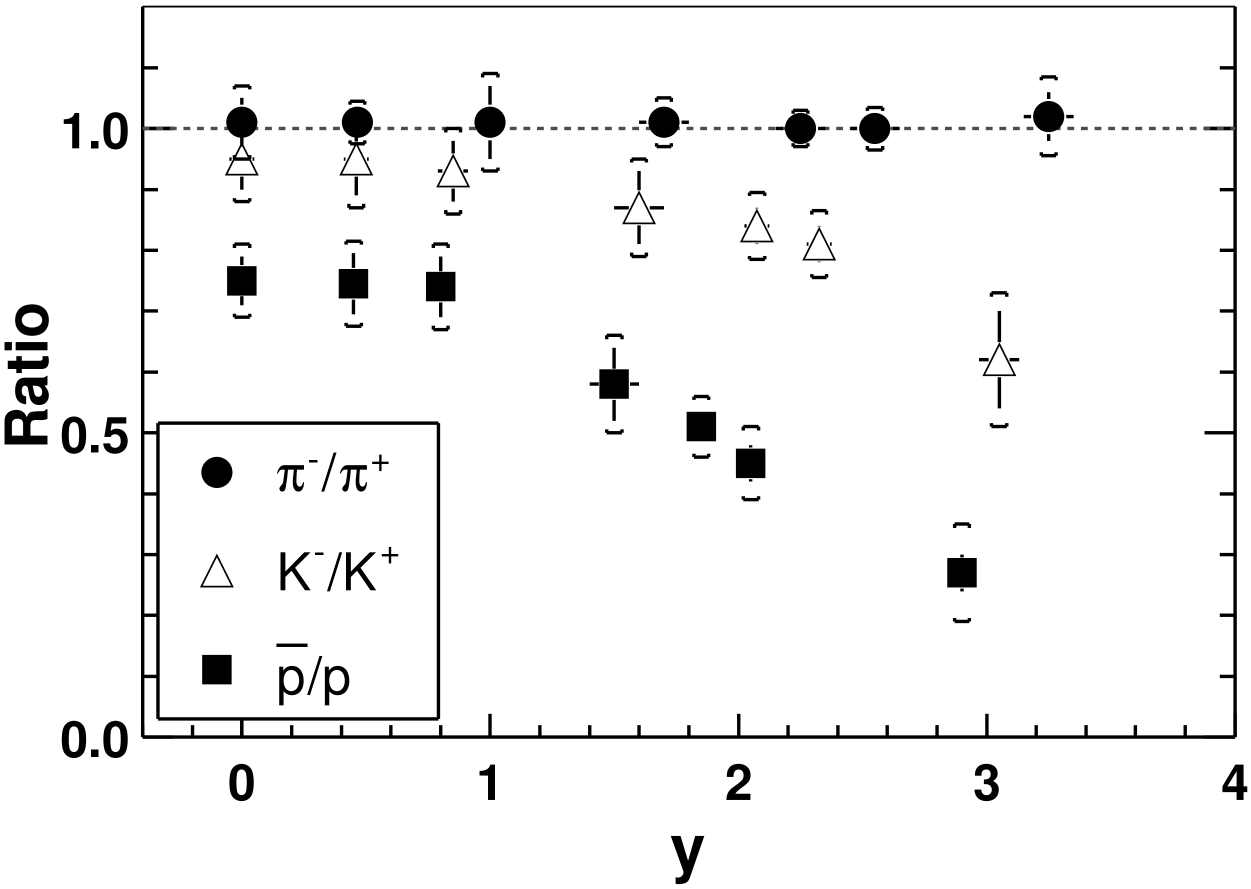

Figure 3: Antiparticle-to-particle ratios as a function of rapidity. The vertical lines show the statistical errors while the caps indicate the combined statistical and systematic errors.

π^-/π^+=1.004. We note the excellent numerical agreement between these calculations and the present measurements. Within this approach the near constancy of the temperature for chemical freeze-out found at
SPS, at lower RHIC energies, and at the present energy can be associated with a fixed deconfinement transition temperature and the establishment of chemical equilibrium during hadronization. The small value of the chemical potential indicates a small net baryon density at midrapidity.

In figure 4 we show the correlation between the K^-/K^+ and $\bar{p}/p$ ratios that we have measured. The ratios are measured at slightly different rapidities. Therefore the K^-/K^+ ratios in fig. 4 are interpolated to the y value of the $\bar{p}/p$ measurements. Also shown are similar ratios determined at AGS [13] and SPS energies [14, 15]. The figure evidences a smooth relationship between the ratios from AGS and SPS to RHIC, that can be expressed by a power law $K^-/K^+ = (\bar{p}/p)^{1/4}$. For vanishing strange-quark chemical potential an exponent of 1/3 would have been expected. Comparison of the two relations indicates the relationship $\mu_s = 1/4 \cdot \mu_q$ for the shown data. Good agreement with the data is also found by comparing the present data with the model of Becattini et al.[19] that is based on extrapolation of SPS results integrated over the full phase space. Within the framework of the statistical model, Fig. 4 therefore suggests, that the particle sources corresponding to the different rapidity regions sampled in our experiments are all in chemical equilibrium with local strangeness conservation and with baryon chemical potentials that decrease from μ_B = 120 MeV at $y \approx 3$ to μ_B = 25 MeV at y=0.

In summary, the BRAHMS experiment has measured the ratios of charged hadrons at the RHIC top energy and observed the highest such ratios yet in nuclear collisions. We find an increase in the ratio of antiprotons to protons and charged singly-strange mesons, consistent with a significant increase in reaction transparency compared to lower energies. The ratios are, within errors, constant in the interval $y = 0 - 1$ suggesting the existence of a boost invariant midrapidity plateau dominated by particle production from the color field. Our ratios are well reproduced by statistical model calculations in which the baryon chemical potential decreases strongly from forward rapidities, where the baryon content of the original colliding nuclei is still significant, towards midrapidity. The systematics of kaon and proton ratios suggests a universal relationship between light and strange quark chemical potentials.

This work was supported by the Division of Nuclear Physics of the Office of Science of the U.S. Department of Energy, the Danish Natural Science Research Council, the Research Council of Norway, the Jagiellonian University Grants, and the Romanian Ministry of Research.

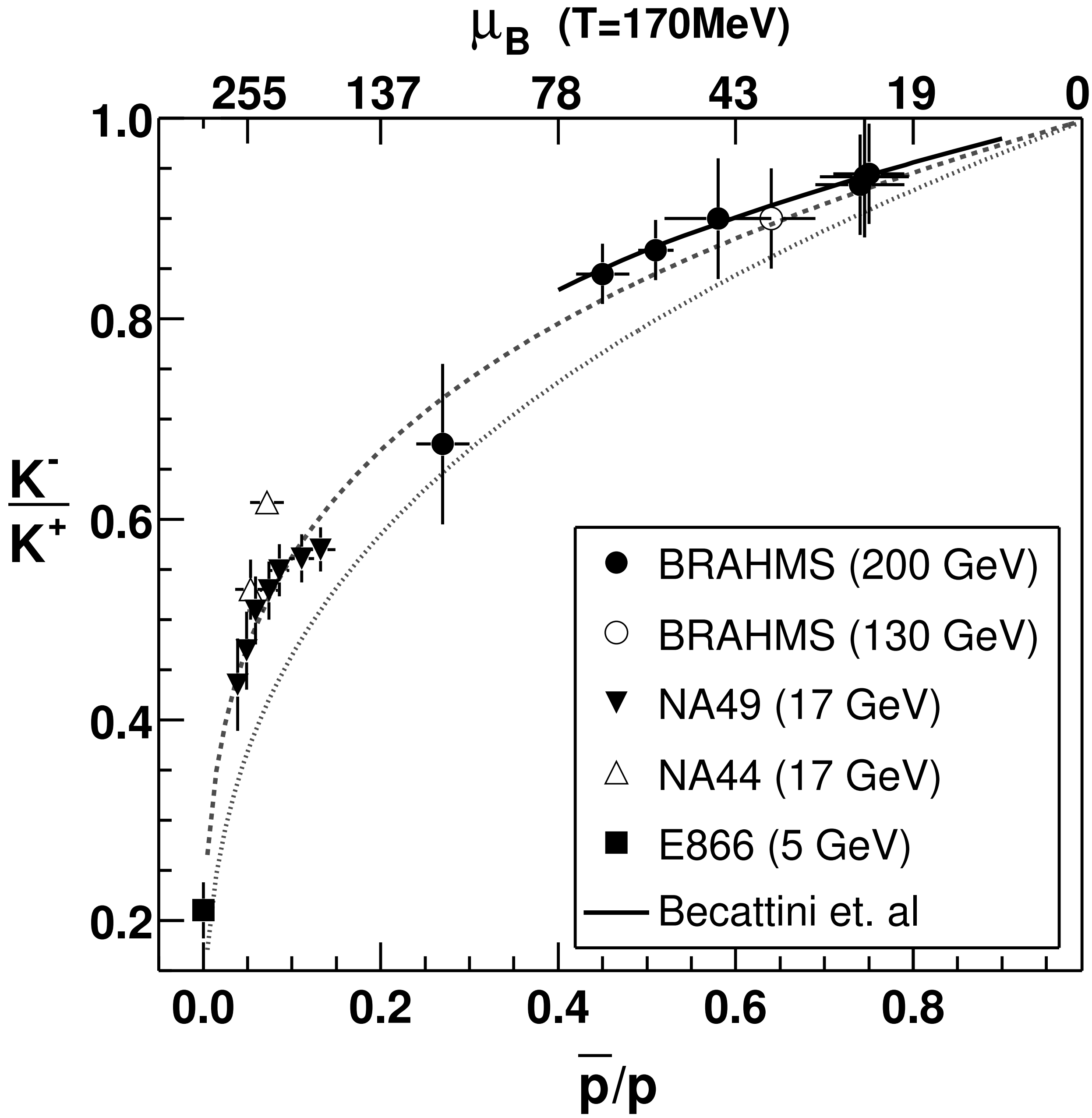

Figure 4: Correlation between strange meson and baryon ratios. The NA44 and NA49 data are from ref.[15] and [14], respectively. The E866 data are from ref.[13]. The dashed line shows the relation $K^-/K^+ = (\bar{p}/p)^{1/4}$ and the dotted line shows $K^-/K^+ = (\bar{p}/p)^{1/3}$. The full line shows the prediction of Becattini et al.[19].

References

[1] N. Herrmann *et al*, Ann. Rev. Nucl. Part. Sci. **49** (1999) 581.

[2] H. Satz. Rep. Prog. Phys. **63** (2000) 1511 .

[3] I. G. Bearden *et al.*, BRAHMS Collaboration Phys. Rev. Lett. **87** (2001) 112305.

[4] C. Adler *et al.*, STAR Collaboration, Phys. Rev. Lett. **86** (2001) 4778.

[5] B. B. Back *et al.*, PHOBOS Collaboration, Phys. Rev. Lett. **87** (2001) 102301.

[6] W. A. Zajc. and PHENIX Collaboration, Nucl. Phys. A698 (2002) 39c.

[7] I. G. Bearden *et al.*, BRAHMS Collaboration, Phys. Lett. B523 (2001) 227.

[8] I. G. Bearden *et al.*, BRAHMS collaboration, Phys. Rev. Lett.88 (2002) 202301.

[9] B. B. Back *et al.*, PHOBOS collaboration, Phys. Rev. Lett. 88 (2002) 022302.

[10] J.D. Bjorken, Phys. Rev. **D27** (1983) 140.

[11] B. B. Back *et al.*, PHOBOS collaboration, Subm to PR Rapid. Comm. (2002), nucl-ex/.

[12] M. Adamczyk *et al.*, BRAHMS collaboration, Nuclear Instruments and Methods, to be published;

[13] L. Ahle et al. E866 Collaboration. Phys. Rev. Lett. 81 (1998) 2650 and Phys. Rev. C60 (1999) 044904.

[14] Y. Afanasiev et al. NA49 Collaboration. Nucl-ex/02050002; J. Bächler et al., Nucl. Phys. **A661**, 45(1999)

[15] I. G. Bearden et al, NA44 collaboration, J. Phys. G, Nucl. Part **23** (1997) 1865 and nucl-ex/0202019.

[16] C. Adler *et al.*, STAR collaboration, Submitted to Phys. Rev. Lett. (2002). Nucl-ex/0203016.

[17] B.Back et.al. Phys. Rev. Lett. **85**(2000) 3100.

[18] P. Braun-Munzinger et al. Phys. Lett. **B518** (2001) 41.

[19] Becattini et al. Phys. Rev. C64 (2001) 024901.